

# Intruder bands and configuration mixing in the lead isotopes

**R. Fossion and K. Heyde**

*Department of Subatomic and Radiation Physics,  
Proeftuinstraat 86, B-9000 Gent, Belgium*

**G. Thiamova**

*Nuclear Physics Institute, Rez, Czech Republic*

**P. Van Isacker**

*GANIL, BP 55027, F-14076 Caen Cedex 5, France*

## Abstract

A three-configuration mixing calculation is performed in the context of the interacting boson model with the aim to describe recently observed collective bands built on low-lying  $0^+$  states in neutron-deficient lead isotopes. The configurations that are included correspond to the regular, spherical states as well as two-particle two-hole and four-particle four-hole excitations across the  $Z = 82$  shell gap.

# 1 Introduction

During the last years, ample evidence for the presence of intruder excitations, in particular at and near closed-shell regions [1, 2] has been accumulated throughout the nuclear mass table. Such intruder excitations, which give rise to shape coexistence and collective band structures, are particularly well documented in the  $Z = 50$  (Sn) and  $Z = 82$  (Pb) mass regions. They can be associated with many-particle many-hole proton excitations across the closed shells [3] but can also be studied, in an equivalent way, using potential energy surface calculations [4].

After the discovery of  $0^+$  intruder excitations in the even-even Pb nuclei, down to mass  $A = 192$  [5–8], the development of recoil and recoil-decay-tagging (RDT) techniques and of heavy-ion induced fusion-evaporation reactions [9] have led to a wealth of new data on collective bands in the Pb isotopes that have neutron number near  $N = 104$ . The large number of experiments carried out over the last few years are described in a review paper by Julin *et al.* [10]. Study of the fine-structure of alpha decay of the very neutron-deficient nuclei has also proven to be an excellent tool [11] to identify excited  $0^+$  states and was used for the first observation of a set of three low-lying  $0^+$  excitations in  $^{186}\text{Pb}$  [12, 13]. The above two major experimental techniques have been instrumental in exploring unexpected new phenomena concerning intruder states and shape coexistence.

With these methods, data have become available on  $^{188}\text{Pb}$  [14–17],  $^{186}\text{Pb}$  [12, 13, 18],  $^{184}\text{Pb}$  [19, 20] and  $^{182}\text{Pb}$  [21]. The experimental evidence for close-lying  $0^+$  excitations and for associated collective band structures (see Fig. 1) has brought about the need to explore and study the effects of mixing among these structures. A first attempt using two-level mixing for the low-lying  $0^+$  and  $2^+$  excitations in  $^{190-200}\text{Pb}$  was carried out by Van Duppen *et al.* [22]. The importance of mixing between bands was put in a broader context by Dracoulis [23] in the Os-Pt-Hg-Pb region. More recently, detailed two-band mixing calculations [24, 25] and an attempt to perform a three-band mixing study in  $^{186}\text{Pb}$  [26] have been reported, albeit all starting from phenomenological band-mixing assumptions. So, there is a clear need to perform a detailed study of these nuclei. We also mention that intruder  $0^+$  states and associated bands have been studied in the neutron-deficient Pt nuclei [27–33] down to mass  $A = 168$  and in the Po nuclei [34–41] in an effort to distinguish collective vibrational excitations from intruder states.

Deformed mean-field calculations [4, 42–44] have indicated the possibility of obtaining oblate and prolate minima close to the spherical ground-state configuration in the total energy surface for the Pb nuclei for neutron numbers close to  $N = 104$ . In the Hg nuclei with a ground state corresponding to a slightly deformed oblate configuration, a second, prolate configuration is predicted with minimal energy near mid-shell ( $N = 104$ ), while in the Pt nuclei a crossing of both minima is found and the prolate deformed minimum becomes the lowest configuration at mid-shell. In the Po nuclei the situation is more complicated [45] with an oblate minimum which approaches the spherical ground-state configuration near  $N = 110$ , and a prolate minimum which becomes dominant in the ground state for even lower neutron numbers. The above studies have the drawback that only the static potential energy surface properties are studied.

Many-particle many-hole ( $mp$ - $nh$ ) excitations cannot be incorporated easily in full large-scale shell-model studies because of the extremely large dimensions of the model spaces involved. These  $mp$ - $nh$  excitations, however, can be handled within an algebraic framework of the Interacting Boson Model (IBM) [46, 47]. The inclusion in IBM of the simplest 2p-2h intruder excitations in the form of two extra nucleon pairs (two bosons) and the study of the mixing with the regular configurations was suggested by Duval and Barrett [48] and applied in the Pb region to the Hg nuclei [49, 50], the Pt nuclei [51] and the Po nuclei [45]. These IBM-mixing calculations, however, generally implied the introduction of many parameters. Calculations including up to 6p-6h excitations have been carried out, using a simplified Hamiltonian, with the aim of studying high-spin properties and backbending within the IBM configuration mixing picture by J. Jolie et al [52, 53]. In an effort to remove the obstacle of introducing many parameters when carrying out such IBM configuration mixing calculations with various  $mp$ - $nh$  excitations, the symmetries connecting particle and hole bosons have been put forward in an algebraic framework and led to the introduction of a new label, called *intruder spin* or  $I$  spin [54] and to applications in the Pb region [55]. In this approach, explored in detail in a series of papers [56–59], both the particle and hole shell-model configurations are handled as interacting particle- and hole-like  $s$  and  $d$  bosons. The method also allows, in principle, the mixing of two dynamical symmetries.

The experimental need to explore three families each with a different intrinsic structure (spherical, oblate and prolate or, in a spherical shell-model

language, the 2p-2h and 4p-4h intruder excitations next to the regular ones of 0p-0h type) forms the starting point of the present study. An exploratory calculation of this kind within an algebraic framework has already been reported [60, 61] but was confined to the  $0^+$  band heads. In this paper an IBM-mixing calculation that describes the three different intrinsic ‘shape’ configurations is performed, and applied to the very neutron-deficient Pb nuclei.

## 2 The configuration mixing model

### 2.1 Hamiltonian

The regular (reg) 0p-0h states are described in terms of  $N$  bosons while the intruder 2p-2h and 4p-4h states require  $N + 2$  and  $N + 4$  bosons, respectively. The model space thus consists of the sum of three symmetric  $U(6)$  representations  $[N] \oplus [N + 2] \oplus [N + 4]$ . The model Hamiltonian has the form

$$\hat{H} = \hat{H}_{\text{reg}} + \hat{H}_{2\text{p}2\text{h}} + \hat{H}_{4\text{p}4\text{h}} + \hat{V}_{\text{mix}}. \quad (1)$$

The different parts are

$$\hat{H}_{\text{reg}} = \epsilon_{\text{reg}} \hat{n}_d + \kappa_{\text{reg}} \hat{Q}_{\text{reg}} \cdot \hat{Q}_{\text{reg}}, \quad (2)$$

$$\hat{H}_{2\text{p}2\text{h}} = \epsilon_{2\text{p}2\text{h}} \hat{n}_d + \kappa_{2\text{p}2\text{h}} \hat{Q}_{2\text{p}2\text{h}} \cdot \hat{Q}_{2\text{p}2\text{h}} + \Delta_{2\text{p}2\text{h}}, \quad (3)$$

$$\hat{H}_{4\text{p}4\text{h}} = \epsilon_{4\text{p}4\text{h}} \hat{n}_d + \kappa_{4\text{p}4\text{h}} \hat{Q}_{4\text{p}4\text{h}} \cdot \hat{Q}_{4\text{p}4\text{h}} + \Delta_{4\text{p}4\text{h}}, \quad (4)$$

with the  $d$ -boson number operator  $\hat{n}_d$  and the quadrupole operator

$$\hat{Q}_i = \left( s^\dagger \tilde{d} + d^\dagger \tilde{s} \right)^{(2)} + \chi_i \left( d^\dagger \tilde{d} \right)^{(2)}, \quad (5)$$

where  $i$  stands for a regular, 2p-2h or 4p-4h configuration. The parameter  $\Delta_{2\text{p}2\text{h}}$  corresponds to the single-particle energy needed to create a 2p-2h excitation, corrected for the gain in binding energy due to pairing. Likewise,  $\Delta_{4\text{p}4\text{h}}$  corresponds to the single-particle energy needed to create a 4p-4h excitation (corrected for pairing), with  $\Delta_{4\text{p}4\text{h}} \approx 2\Delta_{2\text{p}2\text{h}}$ . Eigensolutions depend primarily on the ratio  $\epsilon/\kappa$ . For  $\epsilon \gg \kappa$  the solution is vibrational while for  $\epsilon \ll \kappa$  it is rotational. In addition, the parameter  $\chi$  in the quadrupole operator (5) determines whether the solution is  $SU(3)$  (axially deformed,  $\chi = \pm\sqrt{7/4}$ ) or  $SO(6)$  (triaxially unstable,  $\chi = 0$ ). The Hamiltonians used

in (1) represent the simplest parametrisation of the IBM which encompasses its different limits, U(5) vibrational, SU(3) rotational and SO(6)  $\gamma$  soft. Often a rotational term  $\hat{L}^2$  is added but this is not needed here.

The mixing of the different configurations is induced by  $\hat{V}_{\text{mix}}$ , which is assumed to be of lowest possible order in the  $s$  and  $d$  bosons,

$$\hat{V}_{\text{mix}} = \hat{V}_{\text{mix},1} + \hat{V}_{\text{mix},2}, \quad (6)$$

with

$$\hat{V}_{\text{mix},i} = \alpha_i (s^\dagger s^\dagger) + \beta_i (d^\dagger d^\dagger)^{(0)} + \text{hermitian conjugate}, \quad (7)$$

where  $i = 1, 2$  and  $\hat{V}_{\text{mix},1}$  mixes the regular (0p-0h) and 2p-2h configurations while  $\hat{V}_{\text{mix},2}$  mixes the 2p-2h and 4p-4h configurations. Note that care is taken to introduce different (0p-0h)-(2p-2h) and (2p-2h)-(4p-4h) mixing parameters,  $(\alpha_1, \beta_1)$  and  $(\alpha_2, \beta_2)$ , respectively, and that there is no direct mixing between the 0p-0h and 4p-4h configurations. The latter statement is suggested by the observation that the matrix element of a two-body interaction between 0p-0h and 4p-4h states is zero.

To obtain an estimate of the relation between  $(\alpha_1, \beta_1)$  and  $(\alpha_2, \beta_2)$ , assume in first approximation that the dominant component of the 2p-2h and 4p-4h configurations involves pairs of particles (holes) in a single  $j_p$  ( $j_h$ ) shell coupled to zero angular momentum. For a pairing force the following ratio of mixing matrix elements is obtained:

$$\frac{\langle 0 | \hat{V}_{\text{pairing}} | j_p^2(0) j_h^2(0) \rangle}{\langle j_p^2(0) j_h^2(0) | \hat{V}_{\text{pairing}} | j_p^4(0) j_h^4(0) \rangle} = \frac{1}{2} \sqrt{\frac{(2j_p + 1)(2j_h + 1)}{(2j_p - 1)(2j_h - 1)}} \approx 0.5. \quad (8)$$

In the limit of large shells, the mixing between the 2p-2h and 4p-4h  $0^+$  states is thus twice as strong as that between the ground state and the 2p-2h states. In contrast, the corresponding ratio, obtained with the mixing Hamiltonian (6) and a U(5) vibrational classification of states, equals

$$\frac{\langle s^N | \hat{V}_{\text{mix}} | s^{N+2} \rangle}{\langle s^{N+2} | \hat{V}_{\text{mix}} | s^{N+4} \rangle} = \frac{\alpha_1}{\alpha_2} \sqrt{\frac{(N+1)(N+2)}{(N+3)(N+4)}}. \quad (9)$$

In the limit of large boson number,  $\alpha_2$  should thus be twice as big as  $\alpha_1$  to recover the ratio in eq. (8). In the present application to the Pb isotopes, the

boson number  $N$  is such that the square root in eq. (9) equals about 0.8, by which factor  $\alpha_2$  should be reduced to account for the finite boson number. Another and perhaps more important fact is that both eqs. (8) and (9) are derived for a spherical configuration. It is clear that deformation may drastically change the ratio of mixing matrix elements and, specifically, it may reduce both matrix elements because of the smaller overlap between states with different deformation. Thus the microscopic estimate  $\alpha_2 \approx 2\alpha_1$  cannot be adhered to rigidly and several calculations corresponding to different combinations of mixing matrix elements must be explored.

## 2.2 Parametrisation from known experimental data

### 2.2.1 The regular configuration

In the even-even Pb nuclei,  $126 - N$  valence neutrons form a ground state which is predominantly of seniority zero,  $v = 0$ . This can be viewed as a condensate of neutron pairs coupled to  $0^+$ . Excited states are first built from one broken pair ( $v = 2$ ) with  $2^+, 4^+, 6^+, \dots$ , next two broken pairs ( $v = 4$ )  $0^+, 2^+, 3^+, 4^+, \dots$  and so on. To describe these spherical states in an IBM context, we consider the Hamiltonian (2) with a spherical structure [symmetry limit  $U(5)$ ] and which has  $\epsilon_{\text{reg}}$  as the only parameter. We fix this parameter to the  $2_1^+$  state of the heavier Pb isotopes  $A = 198$  to  $204$ , where the  $mp-nh$  intruder states are high in energy and have little effect on the low-excited spherical states (see fig. 1). We do not consider the one broken pair  $4^+$  ( $g$  boson) or  $6^+$  ( $i$  boson),...states, which can only be described within extended boson models. A constant Hamiltonian for this regular configuration,  $\hat{H}_{\text{reg}} = \epsilon_{\text{reg}} \hat{n}_d$ , yields a constant excitation energy for the  $2_1^+$  state, independent of the number of bosons. The excitation energy of the observed states, however, changes slightly with mass number  $A$  (because of shell effects). We choose  $\epsilon_{\text{reg}} = 0.9$  MeV; this value is a compromise between a  $2_1^+$  state which is somewhat too low and other states that increase too rapidly in energy with angular momentum. A better fixing of  $\epsilon_{\text{reg}}$  could have been obtained by a variation of  $\epsilon_{\text{reg}}$  linear with the number of bosons. For the sake of simplicity this is not done here.

### 2.2.2 The intruder excitations: 2p-2h and 4p-4h configurations

The spectroscopic information on the neutron-deficient Pb isotopes is limited. We use  $I$ -spin symmetry arguments in order to find the IBM parameters of the two intruder configurations in Pb from corresponding bands in neighbouring nuclei where more experimental information is available.

Before deriving the parameters for the 2p-2h configuration in Pb, we first show in fig. 2 the correspondence between the experimental 2p-2h intruder band in  $^{196}\text{Pb}$ —the only Pb isotope where it is known—(left panel) and the intruder analogue regular 0p-4h ground-state band in  $^{192}\text{Pt}$  (middle panel). This 0p-4h band is also shown for other Pt isotopes from mass numbers  $A = 190$  to 200, where the coexisting 2p-6h intruder configuration lies high in energy and has little influence on the 0p-4h band. The right-hand panel of fig. 2 shows an IBM calculation of the 0p-4h band in the Pt isotopes which, using a constant Hamiltonian

$$\hat{H} = \epsilon \hat{n}_d + \kappa \hat{Q} \cdot \hat{Q}, \quad (10)$$

with  $\hat{Q}$  given in eq. (5). The band head of the  $\gamma$  band, the  $2_2^+$  level, is also taken into account in order to restrict the possible parameter values. The parameter  $\chi$  is fixed in order to reproduce the observed ratio  $R$

$$R = \frac{B(E2 : 2_2^+ \rightarrow 0_1^+)}{B(E2 : 2_1^+ \rightarrow 0_1^+)}, \quad (11)$$

which is 0.00732 in  $^{192}\text{Pt}$  [62] and 0.00485 in  $^{194}\text{Pt}$  [63]. Theoretical values are 0.00711 and 0.00500, respectively. It is seen that the experimental spectra for Pb and Pt are very similar up to  $6^+$ . Intruder spin symmetry appears to be a good approximation, and so it seems reasonable to use the 0p-4h parameters of Pt to describe the Pb intruder 2p-2h configuration.

In the same way we derive the parameters for the 4p-4h configuration in Pb. In fig. 3 we show the observed analogue bands of the 4p-4h intruder configuration in the Pb isotopes (left panel), the 2p-6h intruder configuration in the Pt isotopes (second panel) and the regular 0p-8h ground-state configuration in the W isotopes (third panel). In the right-hand panel of fig. 3, an IBM calculation for this 0p-8h band in the W isotopes is shown, with the Hamiltonian (10) again with constant parameters for all isotopes. This calculation also includes the  $2_2^+$  level, the bandhead of the  $\gamma$  band. The parameter  $\chi$  is fixed from the experimental ratio (11) in  $^{182}\text{W}$ , which lies in

the range 0.0252–0.0295 according to the different references in [64]; the calculated ratio is 0.0276. Again,  $I$ -spin symmetry seems to be valid in this case and we use the 0p-8h parameters of W to describe the 4p-4h configuration in Pb.

### 2.3 Three-configuration mixing in the Pb isotopes

With the three parameter sets  $(\varepsilon_i, \kappa_i, \chi_i)$  determined previously for the regular, 2p-2h and 4p-4h configurations, a mixing must now be supplied that reproduces the experimental features of the three-configuration coexistence in the Pb isotopes (the extra parameters  $\alpha_i, \beta_i, \Delta_i$ ). The final set of parameters is given in table 1. In table 2, we present results on the mixing of the three configurations (reg, 2p-2h and 4p-4h, respectively) in the first three  $0^+$  excited states. One clearly notices a rapid stabilization, close to 100%, for the  $0_1^+$  state at the spherical configuration. The  $0_2^+$  and  $0_3^+$  states indicate a strong mixing between the 2p-2h and 4p-4h configurations. Rather quickly, a dominance of the 2p-2h configuration is observed from  $A = 186$  up to heavier masses in the  $0_2^+$  state. In table 3, we identify, for  $^{186}_{82}\text{Pb}_{104}$ , the bands which contain mainly the 2p-2h (called "2p-2h" band) and the 4p-4h (called "4p-4h" band) configuration for a particular  $J_i^\pi$  value. One notices the "4p-4h" band is related to the  $0_2^+$  band head and follows up the  $2_1^+, 4_1^+, 6_1^+, 8_1^+$  states, whereas the "2p-2h" band is connected to the  $0_3^+$  band head and follows up the  $2_2^+, 4_2^+, 6_2^+, 8_2^+$  states, respectively. The results in tables 2 and 3 are particularly illuminating in showing the mixing effects within the IBM configuration mixing.

Note that with constant parameters for all Pb isotopes identical results are obtained for corresponding isotopes that are symmetric around the middle of the shell.

The result of such a mixing calculation is shown in fig. 4 (left panel). From the comparison with the experimental situation, see fig. 4 (right panel), the slope with which the intruder states gain binding energy towards midshell is too steep, an effect that is independent of the mixing. Apparently,  $I$ -spin symmetry is not satisfied completely. A possible cause for these differences between the experimental and theoretical band structures is the fact that the IBM parameters are obtained from separate calculations for the 2p-2h intruder excitations (fig. 2) and 4p-4h intruder excitations (fig. 3). In the final calculation for the even-even Pb nuclei, which includes the 2p-2h and



4p-4h intruder families together with the regular spherical configuration, the extra mixing effects will cause specific perturbations that may show up as a breaking of  $I$ -spin symmetry and may also affect the  $A$ -dependence of the intruder band energies.

Possible improvements can be expected from a more elaborate mixing study, treating *all* known data for the neutron-deficient Pb isotopes and relevant nuclei in the  $Z = 82, N = 126$  region. A further constraint would also be imposed by the condition that the lowest-lying proton 2p-2h  $0^+$  excitations approach the observed energy at  $E_x \approx 4$  MeV in  $^{208}\text{Pb}$ . Such extensive calculations, aiming to describe besides energy spectra and band structures also known electromagnetic (mostly E2 and E0) properties, isotopic and isomeric shifts and nuclear ground-state binding energies, will be pursued in the near future.

Very recently, calculations have been carried out by C. Vargas et al. [65], in order to determine total energy surfaces, starting from the IBM parameters derived in the present paper (see also table 1), using boson coherent states.

### 3 Conclusion

We have explored in the present paper the possibility to describe the co-existence and mixing of three different families of excitations, corresponding to different intrinsic structures as observed in the Pb isotopes. In a mean-field approach the three configurations correspond to spherical, oblate and prolate shapes while in a shell-model description they arise as regular 0p-0h states and 2p-2h and 4p-4h excitations across the  $Z = 82$  proton shell. Previous studies of such three-configuration systems were limited to the  $0^+$  band heads (without the associated bands) either in a mean-field [4, 42–45] or an IBM [60, 61] approach, or, in  $^{186}\text{Pb}$ , to a phenomenological band-mixing calculation [26].

The present description is based on the IBM-configuration mixing approach which was originally proposed for two configurations [48–51]. In an IBM framework the three configurations are described as  $N$ -,  $(N + 2)$ - and  $(N + 4)$ -boson states. To reduce the number of parameters that appear in such a configuration mixing calculation, use is made of the concept of intruder-spin symmetry [54], relating configurations with different numbers of particle ( $N_p$ ) and hole ( $N_h$ ) bosons (i.e., fermion pairs), but with a con-

stant sum  $N_p + N_h = N$ . In this way experimental excitation energies in adjacent Pt and W nuclei are used to fix the essential IBM parameters. The final result is a reasonably good description of the observed bands and their variation with mass number  $A$ . As outlined at the end of section 2.3, ways to improve the present results will need extensive calculations spanning the region of neutron deficient W, Os, Pt, Hg, Pb, Po and Rn nuclei as well as nuclei near the  $Z = 82, N = 126$  doubly-closed shell.

The authors are grateful to M. Huyse, W. Nazarewicz and P. Van Duppen for stimulating discussions on the shell-model interpretation and to J. Jolie and J.L. Wood for help in building the various parts of this description. Financial support of the IWT, the “FWO-Vlaanderen” and the DWTC (grant IUAP #P5/07) is acknowledged. RF also receives financial support from a Marie Curie Fellowship of the European Community (contract number 2000-00084).

## References

- [1] K. Heyde, P. Van Isacker, M. Waroquier, J.L. Wood and R.A. Meyer, Phys. Repts. **102** (1983) 291
- [2] J.L. Wood, K. Heyde, W. Nazarewicz, M. Huyse and P. Van Duppen, Phys. Repts. **215** (1992) 101
- [3] K. Heyde, J. Jolie, J. Moreau, J. Ryckebusch, M. Waroquier, P. Van Duppen, M. Huyse and J.L. Wood, Nucl. Phys. **A446** (1987) 189
- [4] R. Bengtsson, T. Bengtsson, J. Dudek, G. Leander, W. Nazarewicz and Jing-Ye Zhang, Phys. Lett. **B183** (1987) 1
- [5] P. Van Duppen, E. Coenen, K. Deneffe, M. Huyse, K. Heyde and P. Van Isacker, Phys. Rev. Lett. **52** (1984) 1974
- [6] P. Van Duppen, E. Coenen, K. Deneffe, M. Huyse and J.L. Wood, Phys. Lett. **B154** (1985) 354
- [7] P. Van Duppen, E. Coenen, K. Deneffe, M. Huyse and J.L. Wood, Phys. Rev. **C35** (1987) 1861

- [8] P. Dendooven, P. Decrock, M. Huyse, G. Reusen, P. Van Duppen and J. Wauters, Phys. Lett. **B226** (1989) 27
- [9] J. Heese, K.H. Maier, H. Grawe, J. Grebosz, H. Klüge, W. Meczynski, M. Schramm, R. Schubart, K. Spohr and J. Styczen, Phys. Lett. **B302** (1993) 390
- [10] R. Julin, K. Helariutta and M. Muikku, J. Phys. **G27** (2001) R109
- [11] P. Van Duppen and M. Huyse, Hyp. Ints. **129** (2000) 149
- [12] A.N. Andreyev et al., Nature **Vol.405** (2000) 430
- [13] A.N. Andreyev et al., Nucl. Phys. **A682** (2001) 482c
- [14] A.P. Byrne et al., Eur. Phys. J. **A7** (2000) 41
- [15] Y. Le Coz et al., Eur. Phys. J. Direct **A3** (1999) 1
- [16] N. Bijmens et al., Z. Phys. **A356** (1996) 3
- [17] G.D. Dracoulis, A.P. Byrne, A.M. Baxter, P.M. Davidson, T. Kibedi, T.R. McGoran, R.A. Bark and S.M. Mullins, Phys. Rev. **C60** (1998) 014303
- [18] A.M. Baxter et al., Phys. Rev. **C48** (1993) R2140
- [19] A.N. Andreyev et al., Eur. Phys. J. **A6** (1999) 381
- [20] J.F.C. Cocks et al., Eur. Phys. J. **A3** (1998) 17
- [21] D. Jenkins et al., Phys. Rev. **C62** (2000) 021302
- [22] P. Van Duppen, M. Huyse and J.L. Wood, J. Phys. **G16** (1990) 441
- [23] G.D. Dracoulis, Phys. Rev. **C49** (1994) 3324
- [24] G.D. Dracoulis, A.P. Byrne and A.M. Baxter, Phys. Lett. **B432** (1998) 37
- [25] R.G. Allatt et al., Phys. Lett. **B437** (1998) 29
- [26] R.D. Page et al., Eur. Phys. J. (2002) in print

- [27] Y. Xu, K.S. Krane, M.A. Gummin, M. Jarrio, J.L. Wood, E.F. Zganjar and H.K. Carter, Phys. Rev. Lett. **68** (1992) 3853
- [28] D. Seweryniak et al., Phys. Rev. **C58** (1998) 2710
- [29] B. Cederwall et al., Phys. Lett. **B443** (1998) 69
- [30] S.L. King et al., Phys. Lett. **B443** (1998) 82
- [31] F. Soramel et al., Eur. Phys. J. **A4** (1999) 17
- [32] G.D. Dracoulis et al., J. Phys. **G12** (1986) L97
- [33] P.M. Davidson et al., Nucl. Phys. **A657** (1999) 219
- [34] L.A. Bernstein et al., Phys. Rev. **C52** (1995) 621
- [35] W. Younes et al., Phys. Rev. **C52** (1995) R1723
- [36] W. Younes and J.A. Cizewski, Phys. Rev. **C55** (1997) 1218
- [37] N. Fotiades et al., Phys. Rev. **C55** (1997) 1724
- [38] N. Bijmens et al., Phys. Rev. Lett. **75** (1995) 4571
- [39] N. Bijmens et al., Phys. Rev. **C58** (1998) 754
- [40] K. Helariutta et al., Phys. Rev. **C54** (1996) R2799
- [41] K. Helariutta et al., Eur. Phys. J. **A6** (1999) 289
- [42] R. Bengtsson and W. Nazarewicz, Z. Phys. **A334** (1989) 269
- [43] W. Nazarewicz, Phys. Lett. **B305** (1993) 195
- [44] R.R. Chasman, J.L. Egido and L.M. Robledo, Phys. Lett. **B513** (2001) 325
- [45] A.M. Oros, K. Heyde, C. De Coster, B. Decroix, R. Wyss, B.R. Barrett and P. Navratil, Nucl. Phys. **A465** (1999) 107
- [46] F. Iachello and A. Arima, *The Interacting Boson Model* (Cambridge University Press, Cambridge, 1987)

- [47] A. Frank and P. Van Isacker, *Algebraic Methods in Molecular and Nuclear Structure Physics* (Wiley, New York, 1994)
- [48] P.D. Duval and B.R. Barrett, Nucl. Phys. **A376** (1982) 213
- [49] A.F. Barfield, B.R. Barrett, K.A. Sage and P.D. Duval, Z. Phys. **A311** (1983) 205
- [50] A.F. Barfield and B.R. Barrett, Phys. Lett. **B149** (1984) 277
- [51] M.K. Harder, K.T. Tang and P. Van Isacker, Phys. Lett. **B405** (1997) 25
- [52] K. Heyde, P. Van Isacker, J. Jolie, J. Moreau and M. Waroquier, Phys. Lett. **B132** (1983) 15
- [53] K. Heyde, J. Jolie, P. Van Isacker, J. Moreau and M. Waroquier, Phys. Rev. **C29** (1984) 1428
- [54] K. Heyde, C. De Coster, J. Jolie and J.L. Wood, Phys. Rev. **C46** (1992) 541
- [55] K. Heyde, P. Van Isacker and J.L. Wood, Phys. Rev. **C49** (1994) 559
- [56] C. De Coster, K. Heyde, B. Decroix, P. Van Isacker, J. Jolie, H. Lehmann and J.L. Wood, Nucl. Phys. **A600** (1996) 251
- [57] H. Lehmann, J. Jolie, C. De Coster, K. Heyde, B. Decroix and J.L. Wood, Nucl. Phys. **A621** (1997) 767
- [58] C. De Coster, K. Heyde, B. Decroix, J.L. Wood, J. Jolie and H. Lehmann, Nucl. Phys. **A621** (1997) 802
- [59] C. De Coster, K. Heyde, B. Decroix, K. Heyde, J. Jolie, H. Lehmann and J.L. Wood, Nucl. Phys. **A651** (1999) 31
- [60] K. Heyde, J. Schietse and C. De Coster, Phys. Rev. **C44** (1991) 2216
- [61] C. De Coster, B. Decroix and K. Heyde, Phys. Rev. **C61** (2000) 067306
- [62] C.M. Baglin, Nucl. Data Sheets **84** (1998) 813

- [63] E. Browne and B. Singh, Nucl. Data Sheets **79** (1996) 347
- [64] B. Singh and R.B. Firestone, Nucl. Data Sheets **74** (1995) 402
- [65] C. Vargas et al., private communication
- [66] J. Penninga, W.H.A. Hesselink, A. Balanda, A. Stolk, H. Verheul, J. van Klinken, H.J. Riezebos and M.J.A. de Voigt, Nucl. Phys. **A471** (1987) 535
- [67] G.D. Dracoulis et al., Phys. Rev. **C44** (1991) R1246
- [68] B. Cederwall et al., Z. Phys. **337** (1990) 283
- [69] M.J.A. De Voigt et al., Nucl. Phys. **A507** (1990) 472
- [70] D.G. Popescu et al., Phys. Rev. **C55** (1997) 1177
- [71] G. Baldsiefen et al., Nucl. Phys. **A574** (1994) 521
- [72] J. Kantele et al., Phys. Lett. **B171** (1986) 151
- [73] T. Kibedi et al., Nucl. Phys. **A688** (2001) 669
- [74] C.Y. Wu, D. Cline, E.G. Vogt, W.J. Kernan, T. Czosnyka, A. Kavka, R.M. Diamond, Phys. Rev. **C40** (1989) R3

Table 1: Parameters of the IBM-calculation of the three coexisting configurations in the Pb isotopes, as shown in fig. 4. All parameters are in MeV, except for  $\chi$ , which is dimensionless.

configuration	$\epsilon$	$\kappa$	$\chi$	$\Delta$	mixing
regular	0.9	0	—	—	
2p-2h	0.51	-0.014	0.515	1.88	$\alpha_1 = \beta_1 = 0.015$
4p-4h	0.55	-0.020	-0.680	4.00	$\alpha_2 = \beta_2 = 0.030$

Table 2: Magnitudes (in percentages, %) of the three different configurations (reg, 2p-2h, 4p-4h) in the first three  $0_i^+$  states of the Pb isotopes  $186 \leq A \leq 196$ , in the IBM calculation of fig. 4 (left panel).

$0_i^+$	configurations	$^{186}_{82}\text{Pb}_{104}$	$^{188}_{82}\text{Pb}_{106}$	$^{190}_{82}\text{Pb}_{108}$	$^{192}_{82}\text{Pb}_{110}$	$^{194}_{82}\text{Pb}_{112}$	$^{196}_{82}\text{Pb}_{114}$
$0_1^+$	reg	75	93	96	98	99	99
	2p-2h	18	7	4	2	1	1
	4p-4h	7	1	0	0	0	0
$0_2^+$	reg	20	6	4	2	2	1
	2p-2h	27	67	82	89	92	95
	4p-4h	52	27	14	9	6	4
$0_3^+$	reg	4	1	1	-	-	-
	2p-2h	51	28	43	-	-	-
	4p-4h	45	71	57	-	-	-

Table 3: The magnitudes (given in percentages, %) of the three different configurations (reg, 2p-2h, 4p-4h) in the "2p-2h" and "4p-4h" assigned bands of  $^{186}_{82}\text{Pb}_{104}$ , as shown in the IBM calculation of fig. 4 (left panel)

<b>"2p-2h band"</b>				<b>"4p-4h band"</b>			
	reg	2p-2h	4p-4h		reg	2p-2h	4p-4h
$0_3^+$	4	51	45	$0_2^+$	20	27	52
$2_2^+$	5	65	30	$2_1^+$	1	32	67
$4_2^+$	1	77	22	$4_1^+$	0	22	78
$6_2^+$	1	81	18	$6_1^+$	0	17	83
$8_2^+$	0	83	16	$8_1^+$	0	16	84



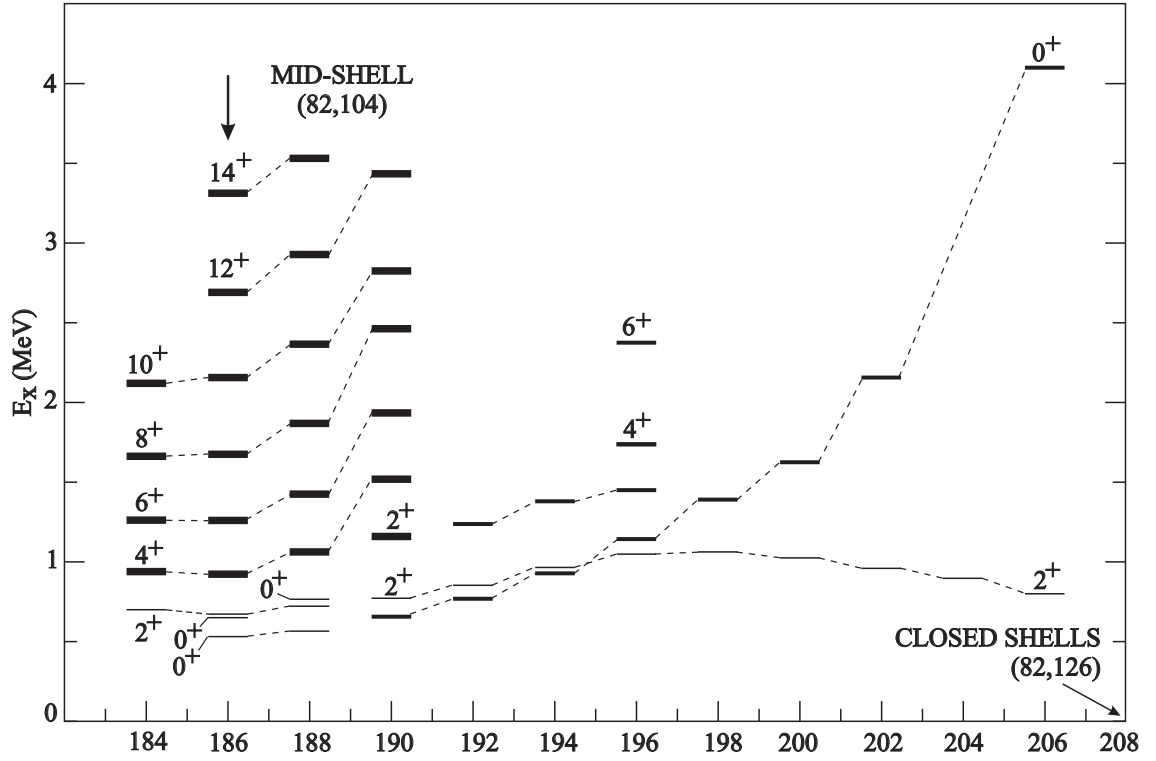


Figure 1: Observed systematics of low-lying  $0^+$  states in even-even Pb nuclei. The first-excited  $2^+$  state is also given for reference and in the mass region  $184 \leq A \leq 190$  known band members of the yrast structure are also shown. This implies that not all observed levels are shown on this figure. References are given in the introduction.

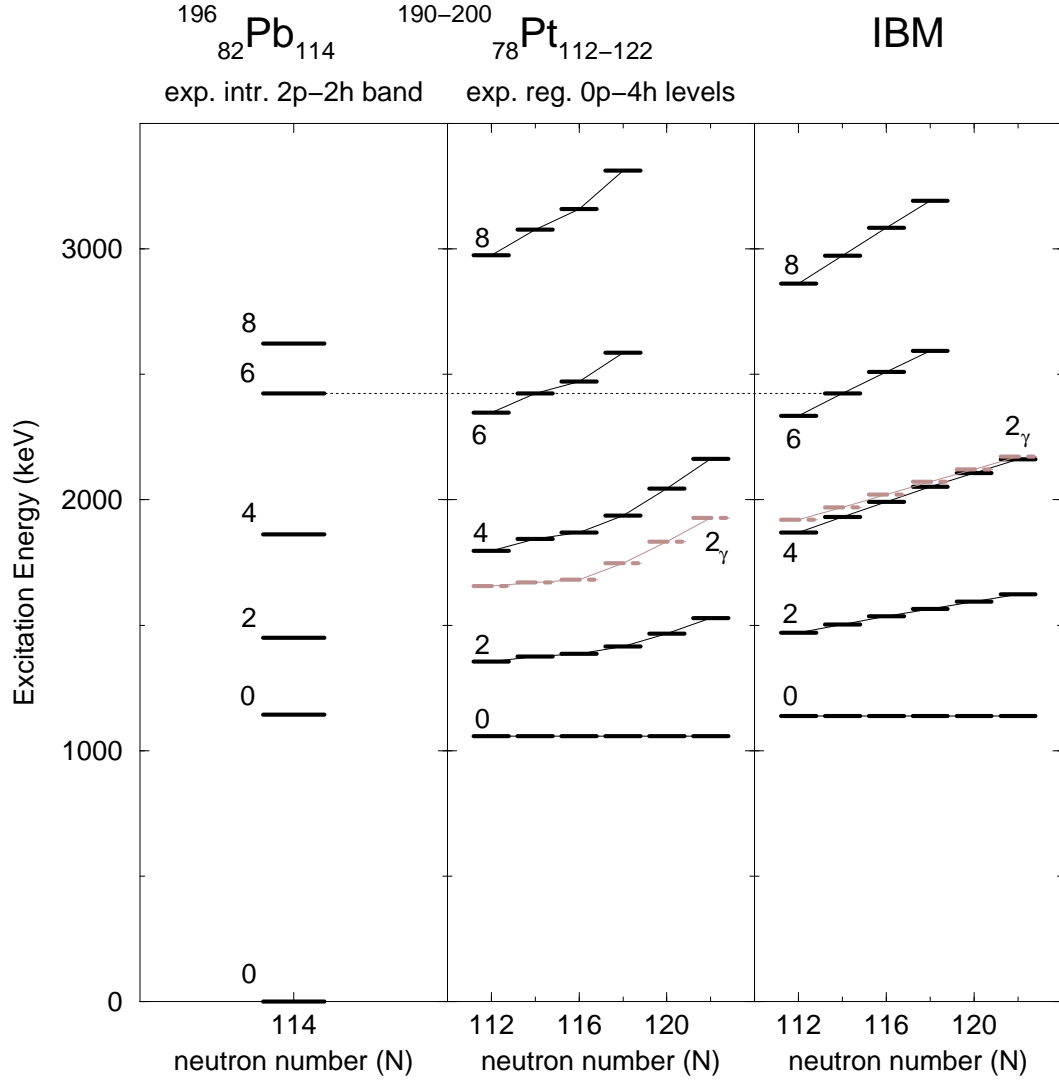


Figure 2: Left panel: Experimental [66] excitation energies of the 2p-2h intruder band in  $^{196}\text{Pb}$  relative to the regular  $0_1^+$  ground state. Middle panel: Experimental [11, 27–33, 51, 67–70] regular (0p-4h) ground-state bands in the Pt isotopes with  $A = 190$  to  $200$ . Right panel: IBM calculation for the Pt isotopes in the same mass range with parameters  $\epsilon = 0.51$  MeV,  $\kappa = -0.0140$  MeV and  $\chi = 0.515$  (kept constant for all isotopes). The Pb and Pt bands are suggested as members of an  $I = 1$  intruder-analog multiplet. Energies in Pt and IBM are normalized to the  $6^+$  excitation energy in the  $N = 114$  isotope and by requiring a constant  $0^+$  energy in other isotopes.

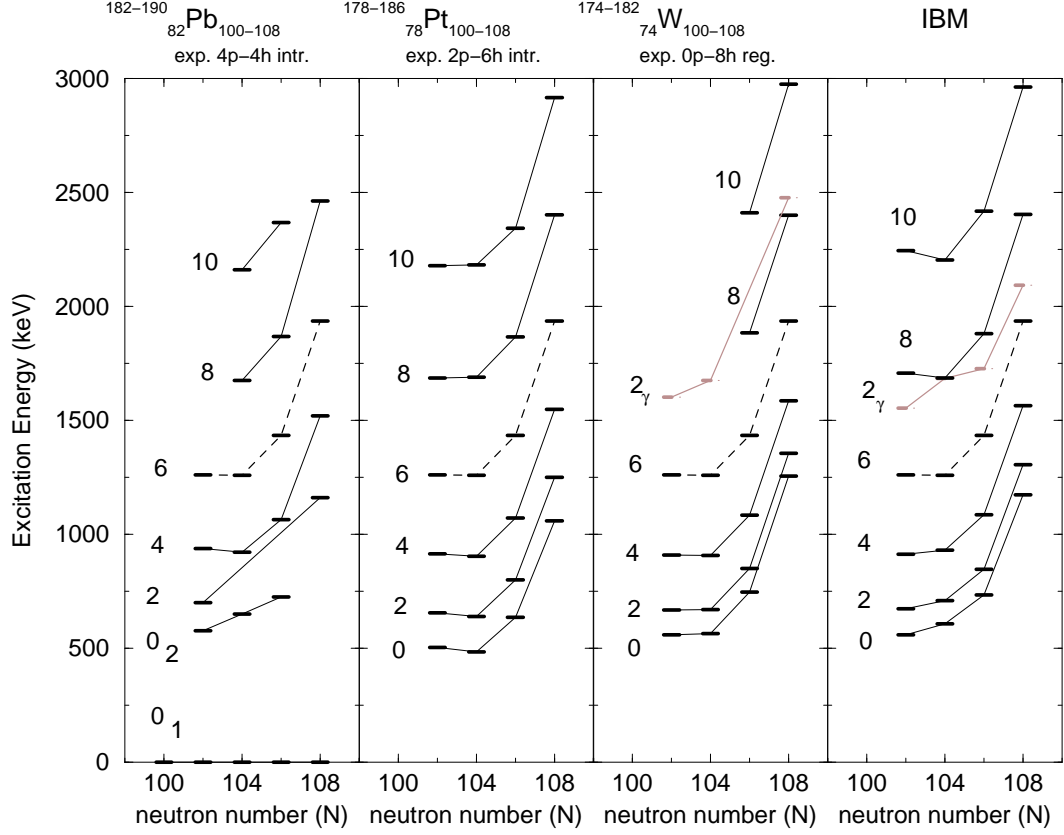


Figure 3: Left panel: Experimental [5–26, 66, 71, 72] 4p-4h intruder bands in the Pb isotopes with  $A = 182$  to 190. Second panel: Experimental 2p-6h intruder bands in the Pt isotopes with  $A = 178$  to 186. Third panel: Experimental [73, 74] regular (0p-8h) ground-state bands in the W isotopes with  $A = 174$  to 182. Right panel: IBM calculation for the W isotopes in the same mass range with parameters  $\epsilon = 0.55$  MeV,  $\kappa = -0.020$  MeV and  $\chi = -0.68$  (kept constant for all isotopes). The Pb, Pt and W bands are suggested as members of an  $I = 2$  intruder-analog multiplet. Energies in Pt, W and IBM are normalized to the  $6^+$  excitation energy in the corresponding Pb isotope.

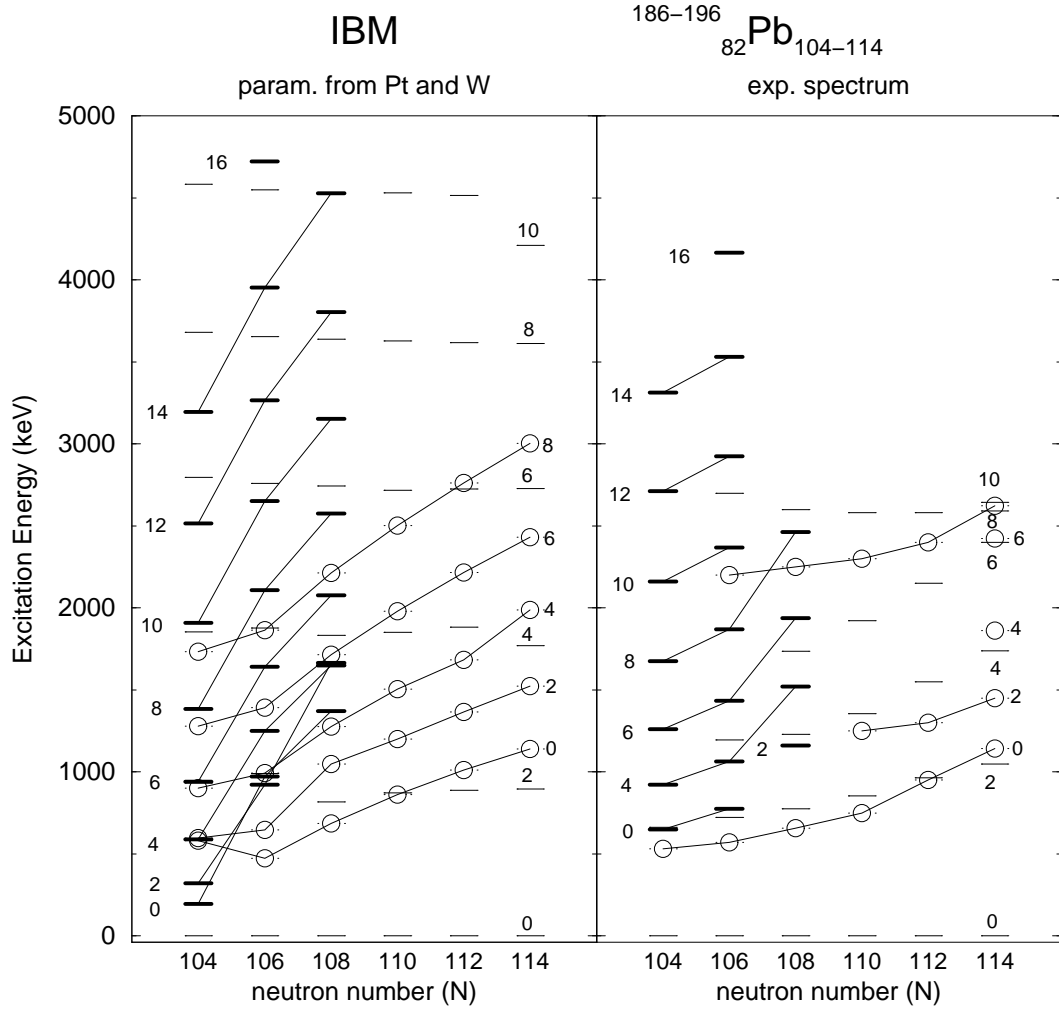


Figure 4: Right panel: Experimental [5–26, 66, 71, 72] spectra of the Pb isotopes with  $A = 186$  to  $196$  containing a regular ground-state spherical band (thin horizontal lines), a 2p-2h intruder band (open circles) and a 4p-4h intruder band (thick horizontal lines). Left panel: IBM calculation for the Pb isotopes in the same mass region, with parameters determined from results obtained in figs. 1-3, as given in table 1.